Large temperature excursions have modest impacts on community composition in the high diversity gut microbiome of omnivorous American cockroaches (*Periplaneta americana*)

Kevin C. Riedmuller[1], Josey E. Dyer[2], Elizabeth A. Ottesen[1]

[1]Department of Microbiology, University of Georgia, Athens, Georgia, United States of America

[2]College of Veterinary Medicine, University of Georgia, Athens, Georgia, United States of America

Abstract

Microbial residents of ectothermic hosts are exposed to variations in temperature that have the potential to impact their physiology and the host-microbe symbiotic relationship. In this experimental warming study, laboratory populations of American cockroaches (*Periplaneta americana*) were kept at a baseline low room temperature of 20-22°C or a high temperature of 30°C for two weeks. We quantified bacterial load and performed high-throughput 16S rRNA gene sequencing to assess the hindgut microbiome's response to a near 10°C shift in environmental temperature. We report modest impacts of temperature on cockroach gut microbiome composition. The high temperature (30°C treatment) induced increases in the relative abundance of Proteobacteria and Euryarchaeota phyla as well as the Lactobacillaceae and Enterococcaceae. We also observed increased interindividual variability. There were no significant differences in the dominant Bacteroidota or Firmicutes phyla and no significant losses or reductions in taxa or bacterial load, respectively. This suggests that the gut community of American cockroaches is largely resilient to prolonged increases in temperature and has implications for the cockroach to withstand the impacts of climate change.

Importance

Insects, as with most animals, often harbor microbial symbionts that play an essential role in host health and nutrition. As insects are ectotherms, these microbial symbionts are subject to the same temperature fluctuations as their hosts, potentially impacting host temperature responses. Here, we demonstrate that the American cockroach (*Periplaneta americana*) gut microbiome exhibits only modest changes following an ~10°C increase in environmental temperature. This contrasts with studies in other insects, whose microbiota were highly

46 responsive to temperature variation. This work illustrates that the microbiota of insects may vary
47 in their sensitivity to long-term temperature shifts, providing a more comprehensive
48 understanding of potential variability in insect responses to climate shifts.
49

50 Introduction

51 Insects are some of the most abundant multicellular organisms on earth with an estimated
52 5.5 million species (1). They are key drivers of ecological and biological processes ranging from
53 nutrient cycling (2,3) to disease dynamics (4,5) and agricultural productivity (6,7). As
54 ectotherms, environmental temperature strongly governs their biological timing, physiology,
55 distribution, and fitness (8). Consequently, changes in environmental temperature can have
56 outsized and varied impacts on insects' roles in these critical systems. For example, simulated
57 warming in mesocosms containing *Formica subsericea*, an ant native to eastern North America,
58 led to decreased decomposition rates and nitrogen availability (9). In contrast, a field study of
59 *Formica Manchu* nests on the southeastern Tibetan Plateau in China found that decomposition
60 rates and nitrogen availability remained stable under simulated warming conditions (10). As
61 2024 was the warmest year on record and global surface temperatures are rising faster than any
62 other period over the last 2000 years (11,12), understanding how insects are affected by warming
63 climate has become increasingly important.
64 Insects have evolved a wide variety of behavioral and physiological thermoregulatory
65 responses for survival that modulate metabolism, stress response, and growth and development
66 (8). Studies frequently report faster growth and/or development rates in response to increased
67 temperature, which is often accompanied by a decrease in body size (13–15). However, one
68 aspect of insect adaptation to temperature that is less well-understood is the impact of

temperature on the insect gut microbiome. The gut microbiome plays a critical role in host nutrition (16–18), development (19–21), and immunity (22–24). As symbionts of ectotherms, gut microbes (and the services they provide to their hosts) are subject to changes in environmental temperature alongside their hosts. Studies in three species of stink bugs have reported reduction or complete loss of gut bacterial symbionts in response to increased environmental temperature by as little as 2.5°C (25,26). Similarly, a paired observational and experimental study in desert arboreal ants found that increased environmental temperature resulted in decreased bacterial loads as well as moderate shifts in microbial community composition. Notably, these changes in the gut microbiome were due to only a 1°C shift from baseline temperature in the experimental treatment (27). These data parallel studies in other ectotherms like corals, sponges, and mussels where increased temperature saw substantial shifts, reductions, or complete loss of symbiotic microbes (28–30). Overall, studies in a variety of invertebrates thus far tend to observe marked changes in both high and low diversity gut microbiomes and subsequent decreases in host fitness as a result of elevated temperatures ranging from ~1-9°C from baseline temperatures.

Omnivorous cockroaches carry a high-diversity hindgut microbiome (31–33) which is believed to play an important role in facilitating host digestion of complex polysaccharides and other refractory dietary components (34,35). The cockroach gut microbiome has been shown to play a vital role in shaping host development (36,37), immune activity (38,39), and behavior (40). It also shows evidence of long-term co-evolution with its host (41) and likely plays a key role in their effectiveness as decomposers and scavengers—functions that contribute significantly to global nutrient cycling due to their ubiquity across terrestrial ecosystems. For example, in central Amazonian inundation forests, at least eight different species of cockroaches

92 were identified, one of which was estimated to consume up to 6% of annual leaf litter (42).
93 Their effectiveness as decomposers and scavengers also contribute to pest species' ability to
94 infest virtually all human spaces (43). Pest species of cockroaches pose significant human health
95 risks as they are a common cause of allergy and asthma (44,45) and vectors for a variety of
96 pathogens (46,47). Moreover, they contribute to economic losses by driving up medical costs
97 (48), destroying property and goods (43), and necessitating continual pest control (49). Given
98 their ecological and economic importance, it is critical that we understand the effects of warming
99 temperatures on the cockroach and its closely associated gut microbiome.

100 While little is known about the impact of temperature on the cockroach gut microbiome,
101 studies of their close relatives the termites (50) show marked temperature impacts. An
102 experimental study in *Reticulitermes flavipes* comparing the gut microbiota at 15°C, 27°C
103 (baseline) and 35°C found dramatic shifts in gut microbiome composition. Colder temperatures
104 were associated with increased relative abundances of Proteobacteria while heat stress was
105 associated with decreased bacterial richness, loss of protist associated bacteria and increased
106 relative abundances of Bacteroidota (51). In contrast, a field study in Janesville, Wisconsin
107 between July and December observed only modest seasonal shifts in gut community composition
108 of *R. flavipes*. However, the mean environmental air temperature during the collection period
109 ranged from 22°C to -2°C, which was substantially lower than the warming treatment in the
110 experimental study (52).

111 The aim of this work was to investigate the impacts of environmental temperature on the
112 gut microbiome of the model insect *Periplaneta americana*. It has been observed that their
113 thermal preference ranges from ~24-33°C (53). However, in many cases experimental insects
114 are kept at a variety of temperatures within or below the thermal preference range (54–56) or at

115 an unspecified room temperature (33,57–59). While such experimental differences likely make
116 little difference to the gut microbiota of endotherms such as mice, it poses a potential
117 complicating factor in studies of microbial symbioses of ectotherms. As a result, we sought to
118 examine the impact of temperature on the gut microbiota of omnivorous cockroaches. To do so,
119 we employed bacterial load quantification and high throughput 16S rRNA gene sequencing to
120 assess the hindgut microbiome's response to an increase in environmental temperature from a
121 'low' laboratory room temperature of 20-22°C to 30°C, a 'high' temperature used to speed
122 reproduction and development (60). This work provides insight into how temperature can
123 impact the gut microbiota of ectothermic hosts; This knowledge has implications for both
124 organismal responses to climate shifts and experimental practice for laboratory investigation of
125 ectotherm symbioses.
126

127 Materials and methods

128 Insects and experimental design

129 *P. americana* cockroach stock colonies have been maintained in captivity at room
130 temperature (20-22°C) for over 15 years. Stock colonies live in 10-gallon glass aquarium tanks
131 with wood chip bedding (PJ Murphy Forest Products SaniChips) and cardboard tubes for
132 housing. They were provided dog chow (Purina One) and water (via cellulose sponge) *ad*
133 *libitum*.
134 For temperature treatments, 20-24 mixed-sex, adult cockroaches were selected from stock
135 colonies, divided into two plastic terrariums, and maintained under stock colony conditions at
136 room temperature (20-22°C) or 30°C for 14 days. Dog chow with any visible mold growth was
137 removed daily. The experiment was performed in duplicate. Cohort 1 and 2 treatments were

138 completed in April of 2022; cohort 2 treatments were initiated one week after cohort 1 began.
139 We also include data from a pilot experiment conducted November of 2020 (cohort 3). The
140 room temperature treatment for this cohort was slightly warmer, ranging from 22-25°C.
141

142 Sample collection and DNA extraction

143 Cockroaches were placed on ice in sterile petri dishes until torpid (~5 min). The entire
144 gut (foregut to rectum) was excised with a scalpel and forceps; any visible fat body and
145 exoskeleton was removed. The gut tract was then moved to a sterile aluminum dish, placed over
146 dry ice, and the hindgut was resected. Hindguts were transferred to 500 µL of sterile 1x
147 phosphate buffered saline and stored at -20°C.
148 Hindguts were thawed and homogenized with a sterile microcentrifuge pestle. DNA was
149 extracted from a 200 µL aliquot of sample homogenate using the E.Z.N.A Bacterial DNA Kit
150 (Omega Bio-tek, Norcross, GA) per manufacturer's protocol with the following modifications:
151 30 min lysozyme incubation, optional glass bead beating step included, and RNase A step
152 excluded. Sample DNA was eluted in 50 µL of elution buffer. DNA concentrations and
153 A260/280 values were measured with a BioTek Synergy HTX Multimode plate reader (Agilent,
154 Santa Clara, CA). Sample DNA was stored at -20°C and concentrations ranged from 30 to 300
155 ng/µL (Table S1).
156

157 Bacterial load quantification

158 Total number of bacteria per sample was assessed via qPCR of the 16S rRNA gene as
159 described in Nadkarni et al. (61). qPCR was performed in triplicate, 10µL reactions using a
160 QuantStudio 6 flex instrument and QuantStudio Real Time PCR Software (v1.3)

161 (Applied Biosystems, Waltham, MA). Reactions consisted of 1x TaqMan Multiplex Master Mix
162 (Applied Biosystems), 0.3 μM forward primer 5′-TCCTACGGGAGGCAGCAGT-3′ (Tm, 59.4
163 °C), 0.3 μM reverse primer 5′-GGACTACCAGGGTATCTAATCCTGTT-3′ (Tm, 58.1 °C), 0.25
164 μM hydrolysis probe (6-FAM)-5′-CGTATTACCGCGGCTGCTGGCAC- 3′-(TAMRA) (Tm,
165 69.9 °C), and 1μL sample DNA (see Table S1 for DNA quantities) under the following
166 conditions: 95°C for 20 s followed by 40 cycles of 95°C for 1 s and 60°C for 60 s. A standard
167 curve was generated with a 10-fold dilution series of gBlocks Gene Fragment of the
168 *Frigididesulfovibrio cuneatus* 16S gene (GenBank: X99503.1, position 330-798) with a linear
169 dynamic range of 10-10^8 copies. The slope, y-intercept, and r^2 of the standard curve was -3.529,
170 41.67, and 0.994, respectively. Amplification efficiency was 92.04%.
171 qPCR of a *Blattabacterium* MIP/aquaporin family protein coding sequence was
172 performed to account for the cockroach endosymbiont's contribution to bacterial load.
173 Triplicate, 10 μL reactions consisted of 1x TaqMan Environmental Master Mix 2.0 (Applied
174 Biosystems), 0.1 μM forward primer 5′-CAGCTAATGCCCATCCCATAG-3′ (Tm, 55.4 °C), 0.1
175 μM reverse primer 5′-GGAAATGGAGTGGTGGCTAAT-3′ (Tm, 55.0 °C), 0.1 μM hydrolysis
176 probe (6-FAM)-5′-TTGTGACCCATCCACCATCTCCAT-3′-(MGB-NFQ) (Tm, 63.7 °C), and
177 1μL sample DNA (see Table S1 for DNA quantities) under the following conditions: 95°C for 10
178 min followed by 40 cycles of 95°C for 15 s and 60°C for 60 s. A standard curve was generated
179 with a 10-fold dilution series of gBlocks Gene Fragment
180 (CAGCTAATGCCCATCCCATAGTGATTGTGACCCATCCACCATCTCCATGTCCTTTTGTT
181 TTAGACAATAGAACATTAGCCACCACTCCATTTCC) with a linear dynamic range of 10-10^8
182 copies. The slope, y-intercept, and r^2 of the standard curve was -3.526, 38.97, and 0.993,
183 respectively. Amplification efficiency was 92.15%.

184 C_q values for both assays were auto selected by the QuantStudio Real Time PCR
185 Software (v1.3). All primers and gBlocks were synthesized by Integrated DNA Technologies
186 with standard desalting purification. Hydrolysis probes were synthesized by Applied
187 Biosystems. Primer set specificity was validated via endpoint PCR and agarose gel
188 electrophoresis.
189 Hindgut bacterial load L was calculated as follows:

190 $$L = ((s - b)/c) \times t$$

191 where $s =$ 16S copy number, $b =$ *Blattabacterium* MIP/aquaporin family protein copy number,
192 $c =$ DNA quantity in qPCR reaction (ng), and $t =$ total sample DNA (ng). Reported 16S and
193 *Blattabacterium* MIP/aquaporin family protein copy numbers are averages from triplicate qPCR
194 reactions. Bacterial load boxplots were generated with the Tidyverse package (62).
195

196 Library preparation and sequencing

197 The V4 region of the 16S rRNA gene from each hindgut sample was amplified using a
198 two-step PCR protocol as described in Tinker et al. (63). Initial amplification of the V4 region
199 was performed with a 10 µL PCR reaction that consisted of 1x Q5 hot start reaction buffer, 0.02
200 U/µL Q5 hot start high-fidelity DNA polymerase (New England BioLabs, Ipswitch, MA), 0.5
201 µM 515F primer 5´-GTGCCAGCMGCCGCGGTAA-3´, 0.5 µM 806R primer 5´-
202 GGACTACHVGGGTWTCTAAT-3´, 200 µM deoxynucleotide triphosphates (dNTPs), and 0.8
203 ng/µL sample DNA under the following conditions: 98°C for 30 s, followed by 15 cycles of
204 98°C for 10 s, 52°C for 30 s, and 72°C for 30 s, followed by a final extension step at 72°C for 2
205 min. The product of reaction 1 was reamplified in a subsequent 30 µL PCR reaction, containing
206 1x Q5 hot start reaction buffer, 0.02 U/µL Q5 hot start high-fidelity DNA polymerase, 0.5 µM

207 515F barcoded primer, 0.5 µM 806R barcoded primer, 200 µM dNTPs, and 9 µL of reaction 1
208 product under the following conditions: 98°C for 30 s, followed by 4 cycles of 98°C for 10 s,
209 52°C for 30 s, and 72°C for 30 s, followed by 6 cycles of 98°C for 10 s and 72°C for 1 min,
210 followed by a final extension step at 72°C for 2 min. All primers were synthesized by Integrated
211 DNA Technologies with standard desalting purification (Coralville, IA).
212 PCR products were verified by agarose gel electrophoresis and purified with the E.Z.N.A
213 Cycle Pure Kit (Omega Bio-tek) per manufacturer's protocol and eluted in 30 µL elution buffer.
214 Purified amplicon concentrations and A260/280 values were measured with a BioTek Synergy
215 HTX Multimode plate reader. Amplicons were normalized and pooled to a final concentration of
216 10 ng/µL. Quality of the prepared amplicon library was assessed with the Agilent 2100
217 Bioanalyzer DNA-HS assay (Agilent) before submission to the Georgia Genomics and
218 Bioinformatics Core for paired-end 250bp sequencing on an Illumina MiSeq platform (Illumina
219 Inc., San Diego, CA).
220

221 **Sequence processing**

222 Demultiplexed, paired-end fastq files were analyzed with the standard DADA2 (64)
223 pipeline. Forward reads were truncated at 240 bp and reverse reads were truncated at 160 bp.
224 Samples were pooled during the sample inference step to increase sensitivity to sequence
225 variants present at low abundances in multiple samples. Taxonomy was assigned to amplicon
226 sequence variants (ASVs) with the DADA2 package and the Silva reference database (v138.1)
227 (65); reads corresponding to *Blattabacterium* (cockroach endosymbiont located in the fat body),
228 chloroplasts, and mitochondria were removed. All downstream analyses of sequencing and

229 bacterial load data were performed using R Statistical Software (v4.2.1) (66) and Geneious
230 Prime 2025.0.3 (https://www.geneious.com).
231

232 Alpha and beta diversity

233 All libraries were resampled to a depth of 10,797 reads with the Vegan package (v2.6-4)
234 (67) for alpha and beta diversity metrics. Alpha diversity was assessed by calculating the
235 Shannon diversity index, richness (number of observed taxa), and Pielou's evenness (Shannon
236 diversity index/log(richness)) (67). Alpha diversity was visualized with violin plots via the
237 Tidyverse packages (v2.0.0) (62). Beta diversity was assessed by calculating weighted and
238 unweighted (incidence based, equivalent to Sorenson index) (68) Bray-Curtis dissimilarities (67).
239 Beta diversity was visualized with nonmetric multidimensional scaling ordinations and violin
240 plots via the Tidyverse and Vegan packages (62,67).
241

242 Differential abundance analysis

243 DESeq2 (v1.38.3) (69) was implemented for ASV level differential abundance analysis to
244 identify temperature responsive taxa. The ASV raw counts table was passed to the DESeq
245 command with default parameters and 'design = ~ cohort + temperature', testing for the effect of
246 temperature while controlling for cohort variation. ASVs with an adjusted p value < 0.05 were
247 considered significant (Table S2). A phylogenetic tree of differentially abundant ASVs present in
248 the 12 most abundant families (maximum relative abundance > 10%) was generated in Geneious
249 Prime. Sequences were aligned with Clustal Omega (v1.2.3) (70) and the phylogenetic tree was
250 built using FastTree (v2.1.11) (71,72). The *Desulfovibrionaceae* clade was used as an outgroup
251 for rooting, and tree visualization was performed in R with the Tidyverse and ggtree (v3.6.2) (73)

252 packages. A heatmap of differentially abundant ASVs present in the 12 most abundant families
253 was generated with the ComplexHeatmap package (74,75).
254

255 Data availability

256 The sequences generated from this experiment were submitted to the NCBI Sequence Read
257 Archive and are available under BioProject PRJNA1380472.
258

259 Results

260 Hindgut bacterial load is stable across temperature treatments.

261 To assess the effect of temperature on hindgut bacterial load, we performed qPCR of the
262 16S rRNA gene with a universal primer/probe set as described in Nadkarni et al (61). To account
263 for 16S rRNA copy contribution from the cockroaches' *Blattabacterium* endosymbiont, we also
264 performed qPCR of a *Blattabacterium* gene in the MIP/aquaporin family. Wilcoxon rank-sum
265 tests, a non-parametric test comparing the distribution of independent groups, were used for two-
266 group comparisons. Kruskal-Wallis tests, an extension of the Wilcoxon rank-sum test, were used
267 for the overall comparison of three or more groups (non-parametric ANOVA analogue).
268 Significant Kruskal-Wallis tests were followed up with post-hoc Dunn's test with Bonferroni
269 adjustment to determine which groups' distributions were significantly different (FSA v0.9.6)
270 (76). A Wilcoxon rank-sum test found no significant difference in hindgut bacterial load across
271 temperature treatments ($p = 0.26$). A Kruskal-Wallis test found a significant difference in
272 hindgut bacterial load among cohorts ($p = 0.04$). However, Dunn's test did not indicate

273 significant differences between cohorts: cohort 1 and 2 ($p = 0.10$), cohort 1 and 3 ($p = 1.00$), and
274 cohort 2 and 3 ($p = 0.07$) (Fig 1).
275

276 Hindgut microbial community composition

277 A total of 4,526,160 rRNA gene sequences were obtained and 2,580,005 passed filtering
278 parameters, resulting in an average of 42,295 reads per sample. One sample was removed prior
279 to downstream analysis due low sequencing depth (Table S3). 2,923 unique ASVs were
280 identified across all samples.
281 Overall gut microbiome composition exhibited modest changes in response to
282 temperature. Wilcoxon rank sum tests found no significant differences in the Shannon diversity,
283 Pielou's evenness, or richness (total number of ASVs) of samples at the ASV or family level
284 across temperature treatments (Shannon: ASV $p = 0.86$, family $p = 0.57$; Pielou's: ASV $p = 0.88$,
285 family $p = 0.56$; richness: ASV $p = 0.64$, family $p = 0.47$) (Figs 2A and S1A). However, beta
286 diversity measures suggest modest but significant impacts of temperature on gut microbiome
287 community composition. Dunn's test indicated that between-temperature treatment
288 dissimilarities were significantly greater than within- room temperature treatment dissimilarities
289 at the ASV ($p < 0.001$) and family level ($p < 0.001$) (Figs 2B and S1B). While nonmetric
290 multidimensional scaling (NMDS) of weighted Bray-Curtis dissimilarities did not indicate clear
291 separation of samples by temperature, permutational multivariate analysis of variance
292 (PERMANOVA) (67) found a significant effect at the ASV ($p = 0.001$, $r^2 = 0.05$) and family ($p =$
293 0.001, $r^2 = 0.05$) levels (Figs 2C and S1C). Temperature was also observed to have impacts on
294 beta dispersion, with the 30°C treatment having higher within-group dissimilarity than the room
295 temperature treatment (Dunn's test: ASV $p < 0.001$, family $p < 0.001$) (Figs 2B and S1B).

296 Given the large time gap between experiments, we also examined cohort impacts on
297 community composition. Notably, cohort 3 samples tended to cluster separately from other
298 cohorts by weighted and unweighted Bray-Curtis metrics and PERMANOVA found a significant
299 effect for cohort on community composition at the ASV (weighted: $p = 0.001$, $r^2 = 0.07$;
300 unweighted: $p = 0.001$, $r^2 = 0.13$) and family (weighted: $p = 0.04$, $r^2 = 0.04$, unweighted: $p =$
301 0.001, $r^2 = 0.22$) level (Figs 2C and S1C). Dunn's test indicated significantly greater between-
302 cohort dissimilarity for all comparisons involving cohort 3 compared to the between-cohort
303 dissimilarity of 1 and 2 by weighted and unweighted metrics at the ASV level ($p < 0.001$) (Fig
304 S2). This suggests that some observed taxa in cohort 3 differ from the observed taxa in cohorts 1
305 and 2. This trend aligns temporally with each experiment, where cohort 1 and 2 treatments were
306 carried out within a week of each other while cohort 3 was carried out over one year earlier. This
307 indicates minor, detectable drift in taxonomic composition of our stock colonies. To investigate
308 whether cohort effects were obscuring temperature responses, we examined temperature effects
309 on gut microbiome composition separately for cohorts 1 and 2, which were combined due to
310 their more similar community composition, and cohort 3 (Figs 2C and 3). Accounting for cohort
311 variation, samples separated more clearly by temperature at the ASV level (weighted Bray-Curtis
312 dissimilarity) than at the family level (Fig 3), although the effect size of temperature calculated
313 by PERMANOVA was still modest (cohort 1 and 2: $p = 0.003$, $r^2 = 0.07$, cohort 3: $p = 0.001$, $r^2 =$
314 0.13). This suggests that, while we observe stability of the gut microbiome at the family-level in
315 response to temperature, there may be some ASV-level differences contributing to observed
316 stability.
317
318

Taxa exhibiting significant responses to temperature differences

All ASVs present in more than 50% of the room temperature samples were also present in the 30°C samples, and vice versa, suggesting that temperature differences in community composition were primarily the result of changes in ASV relative abundance. We performed differential abundance analysis with DESeq2 to further explore ASV level responses to environmental temperature. Accounting for cohort variation, 231 ASVs were identified as significantly differentially abundant ($p < 0.05$) across temperature treatments (Table S2). Of those 231 ASVs, 123 belonged to the most abundant families (maximum relative abundance > 10%) in our samples (Figs 4 and S4). Ruminococcaceae and Lachnospiraceae families had a comparable number of ASVs enriched in both temperature treatments. This may be indicative of ASV-level switching among functionally redundant taxa within these families. However, we did not see this trend for the remaining families. All but one Bacteroidaceae ASV was enriched in the room temperature treatment and all Lactobacillaceae and Enterococcaceae ASVs were enriched in the 30°C treatment. We found that most differentially abundant ASVs in the Tannerellaceae, Dysgonomonadaceae, Rikenellaceae, Christensenellacae, and Desulfovibrionaceae families were enriched in the 30°C treatment (Figs 4 and S4).

These ASV level differences translated into significant differences in family and phylum level abundances. At the family level, Wilcoxon rank sum tests found that Bacteroidaceae were significantly more abundant at room temperature (median difference = 2.07%, $p < 0.001$) while Lactobacillaceae and Enterococcaceae were significantly more abundant at 30°C (median difference = 1.94%, $p = 0.01$ and median difference = 0.41%, $p = 0.005$) (Figs 5A and S5). When summed at the phylum level, Bacteroidota and Firmicute (Bacillota) abundances were not significantly different across temperature treatments ($p = 0.83$ and $p = 0.89$). In contrast, the

342 sulfate-reducing Desulfobacterota (Thermodesulfobacteridota) were significantly more abundant
343 at room temperature (median difference = 3.5%, $p = 0.04$) while the Euryarchaeota (containing
344 exclusively *Methanibrevibacter* ASVs) were significantly more abundant at 30°C (median
345 difference = 0.17%, $p = 0.005$). Proteobacteria were significantly more abundant in the 30°C
346 treatment (median difference = 0.26%, $p = 0.04$) (Figs 5B and S6).
347

348 # Discussion

349 The goal of this study was to examine how changes in environmental temperature affect
350 gut microbial community composition and stability in omnivorous cockroaches. We observed
351 modest differences between room temperature (20-22°C) and 30°C treatments at the phylum and
352 family level (Figs 2 and S1). At the phylum level, there were significantly more Proteobacteria
353 in the 30°C treatment than the room temperature treatment. The observed shift in Proteobacteria
354 relative abundance was subtle, with a median difference of 0.26% (Fig S1). This response
355 parallels studies in other insects and invertebrates. In a study of rough wood lice (*Porcellio*
356 *scaber*), those maintained at 22°C had higher abundances of Proteobacteria (Enterobacteriaeae)
357 compared to those maintained at 15°C (77). Experimental warming of the invertebrate nematode
358 *Caenorhabditis elegans* also resulted in higher abundances of Proteobacteria (*Agrobacterium*) as
359 temperature increased (15, 20, and 25°C treatments) (78). However, those studies observed more
360 pronounced changes in Proteobacteria abundances compared to our findings in the American
361 cockroach and were concurrent with substantial decreases in other common gut microbiota such
362 as the Actinobacteria in *P. scaber* and *Sphingobacterium* in *C. elegans*. In the closely related
363 termite *Reticulitermes flavipes*, Arango et al. saw a considerable increase in the abundance of
364 Proteobacteria (*Acinetobacter,* Betaproteobacteriales, *Enterobacter*) at their lowest temperature

365 treatment of 15°C compared to 27 or 35°C as well as subsequent decreases in Bacteroidota
366 abundances (51). Studies in the fruit fly *Drosophila melanogaster* and cricket *Gryllus veletus*
367 also report that Proteobacteria are responsive to temperature (79,80). However, the responsive
368 Proteobacteria in the fruit fly and cricket studies are primarily *Wolbachia*, an intracellular
369 bacterial symbiont that is not directly associated with the gut microbiome.

370 In vertebrate studies, increases in Proteobacteria abundance are associated with gut
371 dysbiosis, pronounced shifts in community composition and diseases like irritable bowel
372 syndrome and Crohn's disease (81–83). The Proteobacteria are generally composed of
373 opportunists that can survive a broad range of stressors compared to other phyla. It may be that
374 changes in their abundance is indirectly determined by other community members response to
375 temperature. In this scenario, Proteobacteria are well suited to 'take over' under conditions where
376 more typical symbiotic populations are under environmental stress. We observed similar patterns
377 with the Enterococcaceae and Lactobacillaceae in the 30°C treatment (Figs 4, 5 and S4), both of
378 which are also commonly associated with gut dysbiosis (84,85). These taxa appear to bloom in a
379 subset of our 30°C samples, consistent with our observation of increased beta-dispersion under
380 high temperature conditions. This aligns with the "Anna Karenina" model where dysbiotic
381 microbiota are unique and highly variable compared to healthy microbiota (86,87). We note a
382 similar pattern in *Cephalotes rohweri* ant colonies exposed to high temperatures in field warming
383 studies (27).

384 We also observed a significant decrease in Desulfobacterota at higher temperatures. The
385 Desulfobacterota are highly active in *P. americana*, primarily acting as sulfate reducers (34,88).
386 As sulfate reducers, they are likely in competition with methanogens for hydrogen (89,90).
387 Cockroach gut methanogenic taxa include the Euryarchaeota which were significantly more

388 abundant in the 30°C treatment. This suggests that hydrogen utilization may tip in favor of
389 methanogens at higher temperatures, or that methanogens themselves fare better at higher
390 temperatures, increasing hydrogen utilization and decreasing Desulfobacterota abundances.
391 These observations align with studies in soils and batch reactors, where methanogens
392 outcompete sulfate reducers as temperatures rise (91–93). Further studies are needed to better
393 quantify the methanogenic archaea, as universal 16S rRNA primers used in this study are not
394 optimized for their detection.

395 The modest shifts in gut microbiome composition that we report here contrasts with the
396 experimental warming of *R. flavipes* termites, in which a shift from 27°C to 35°C resulted in
397 large changes in phylum-level composition. Arango et al. reported that Bacteroidetes
398 (Bacteroidota) almost doubled in relative abundance while Spirochaetes, Euryarchaeota and
399 Elusimicrobia decreased. However, the authors noted that many of the microbial taxa lost
400 following warming tended to be associated with ciliated protists that do not fare well at these
401 higher temperatures (51). These protists are critical for breakdown of lignocellulosic material in
402 lower termites (94). While similar protists have been reported in the cockroach, they are not
403 essential for cockroach survival and energy acquisition (95). Microscopic observation of
404 samples from our stock tanks indicate that a few protists are present but that they tend to be
405 present at low abundance and low frequency. It may be that the 'high' temperature tested here
406 was not high enough to negatively impact the protists, or that any reduction in protists had a
407 negligible impact on overall community composition.

408 Together, these results suggest that the cockroach gut microbiome is relatively stable
409 across a wide range of environmental temperatures. While the 30°C temperature used in our
410 study is within the preferred temperature range of this species, we observed that all cockroaches

411 maintained at this temperature had a darker cuticle by the end of the experiment. Cuticle
412 melanization has been directly linked to dessication tolerance in *Blattella germanica* (96),
413 suggesting that our warming treatment was high enough to elicit a melanization stress response
414 in *Periplaneta americana*. Additionally, it is common for bacteria to have lower tolerances for
415 higher-than-preferred than lower-than-preferred temperatures (97). The high temperature tested
416 shows some signs of increased variability and growth of opportunistic Proteobacteria,
417 Enterococcaceae, and Lactobacillaceae which may have implications for the ability of these
418 insects to serve as disease vectors in less climate-controlled settings. Finally, we highlight the
419 potential for temperature to impact microbial competition between essential hydrogenotrophic
420 organisms in the gut. This study suggests that the microbiome of ectotherms can be surprisingly
421 resilient to temperature shifts of up to 10°C and has important implications for the ability of
422 these insects to tolerate the impacts of climate change.
423

424 # Acknowledgements

425 This work was supported by the National Institute of General Medical Sciences of the National
426 Institutes of Health under award number R35GM133789 and the National Science Foundation
427 Graduate Research Fellowship Program under Grant No. 2236869. Any opinions, findings, and
428 conclusions or recommendations expressed in this material are those of the author(s) and do not
429 necessarily reflect the views of the National Science Foundation.
430
431
432
433

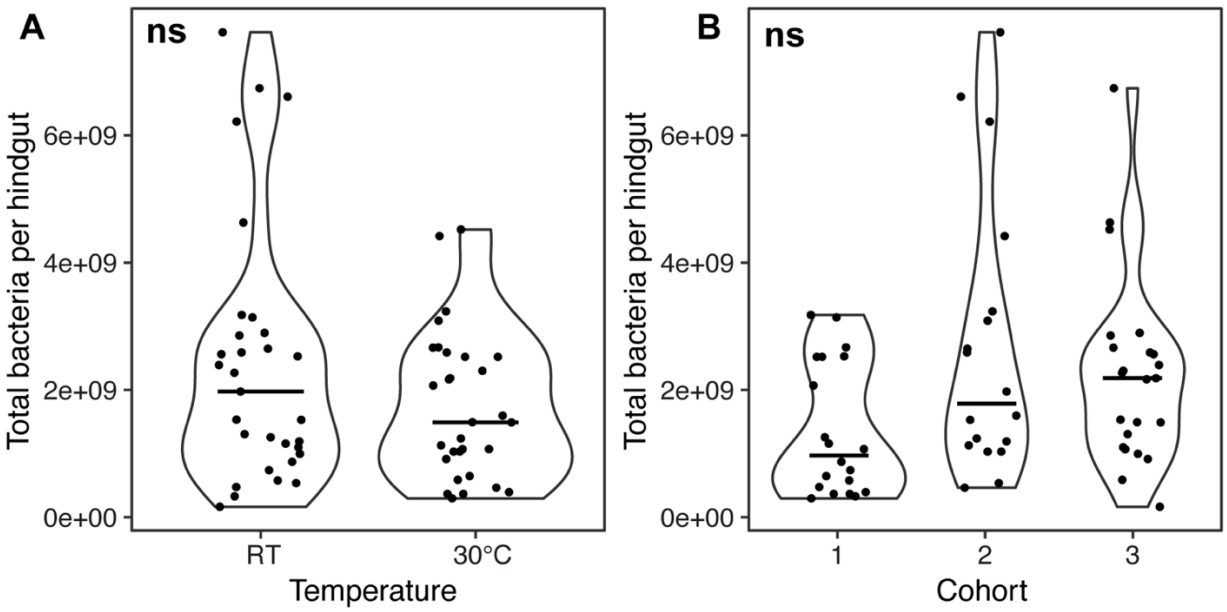

Fig 1. Comparison of hindgut bacterial load across temperature treatments and cohort. Violin plots of hindgut bacterial load across (A) temperature and (B) cohort where bars represent the median and points represent individual samples. Wilcoxon rank-sum test was used to compare across temperature treatments. Kruskal-Wallis and post-hoc Dunn's test with Bonferroni adjustment was used to compare across cohorts. *Blattabacterium* counts subtracted from total 16S rRNA copy number. Bacterial load normalized by total sample DNA. RT = room temperature, ns = no significance.

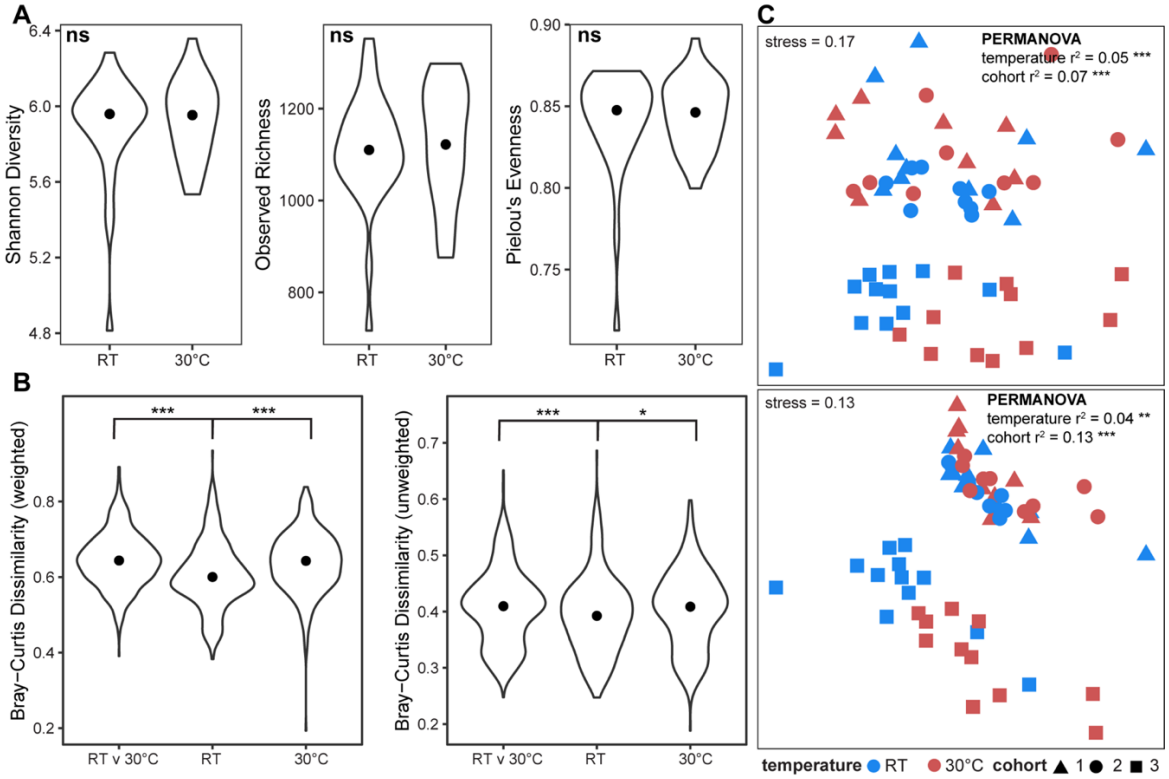

Fig 2. ASV level comparison of hindgut microbial community composition across temperature treatments.

(A) Violin plots of alpha diversity measurements (Shannon diversity, observed richness, Pielou's evenness) where points represent the medians. (B) Violin plots of weighted (left) and unweighted (right) Bray-Curtis dissimilarities within and between temperature treatments where points represent the medians. Wilcoxon rank-sum tests were used to compare alpha diversity measures. Kruskal-Wallis and post-hoc Dunn's test with Bonferroni adjustment was used to compare Bray-Curtis dissimilarities. (C) Nonmetric multidimensional scaling (NMDS) of weighted (top) and unweighted (bottom) Bray-Curtis dissimilarities. NMDS stress was calculated with the metaMDS() function from the Vegan package. PERMANOVA was used to calculate r^2 and p values for temperature and cohort. All libraries were resampled to a depth of 10,797 reads. RT = room temperature, * = $p < 0.05$, ** = $p < 0.01$, *** = $p < 0.001$, ns = no significance.

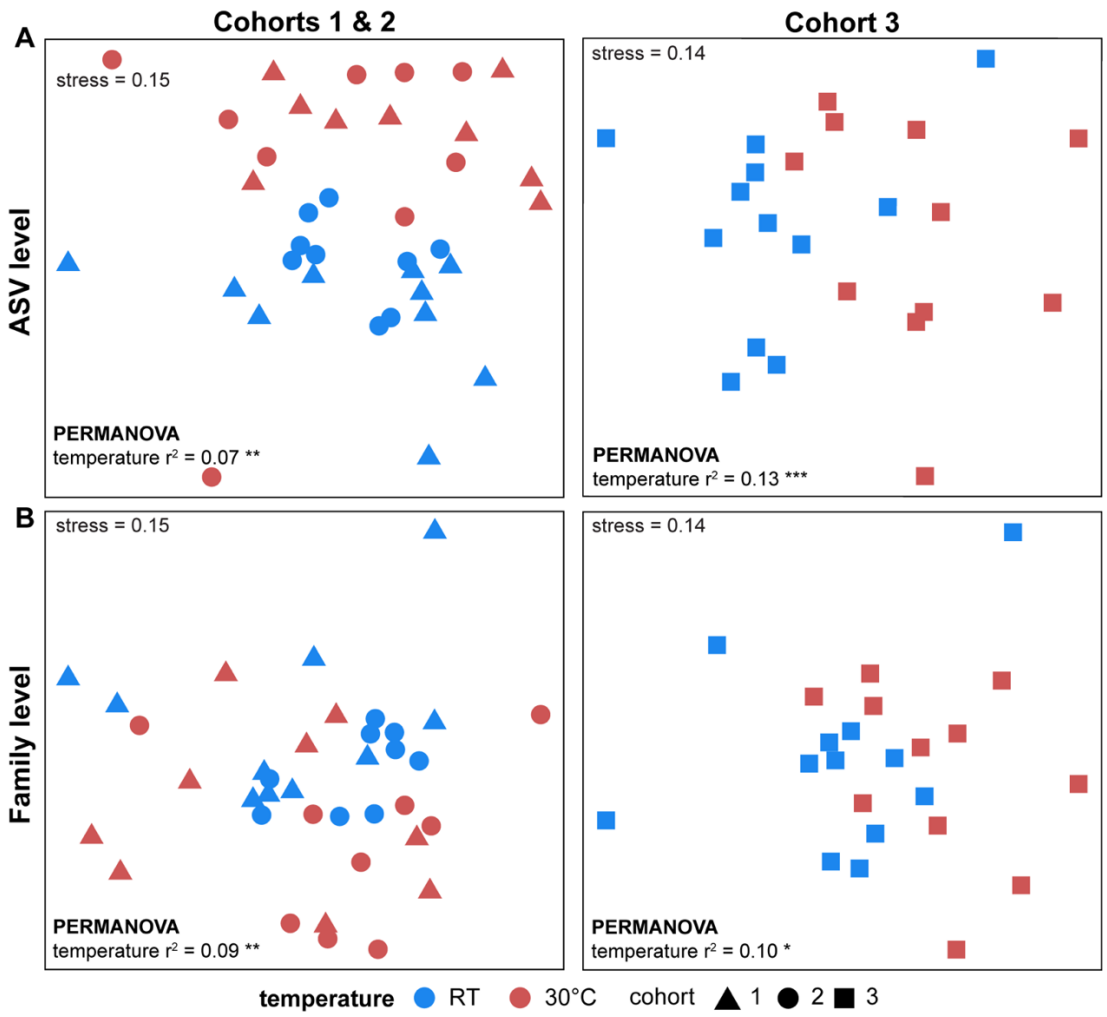

Fig 3. ASV and family level comparison of Bray-Curtis dissimilarities accounting for cohort differences.

Nonmetric multidimensional scaling (NMDS) of weighted Bray-Curtis dissimilarities at the (A) ASV and (B) family level. NMDS stress was calculated with the metaMDS() function from the Vegan package. PERMANOVA was used to calculate r^2 and p values for temperature and cohort. All libraries were resampled to a depth of 10,797 reads. RT = room temperature, * = $p < 0.05$, ** = $p < 0.01$, *** = $p < 0.001$.

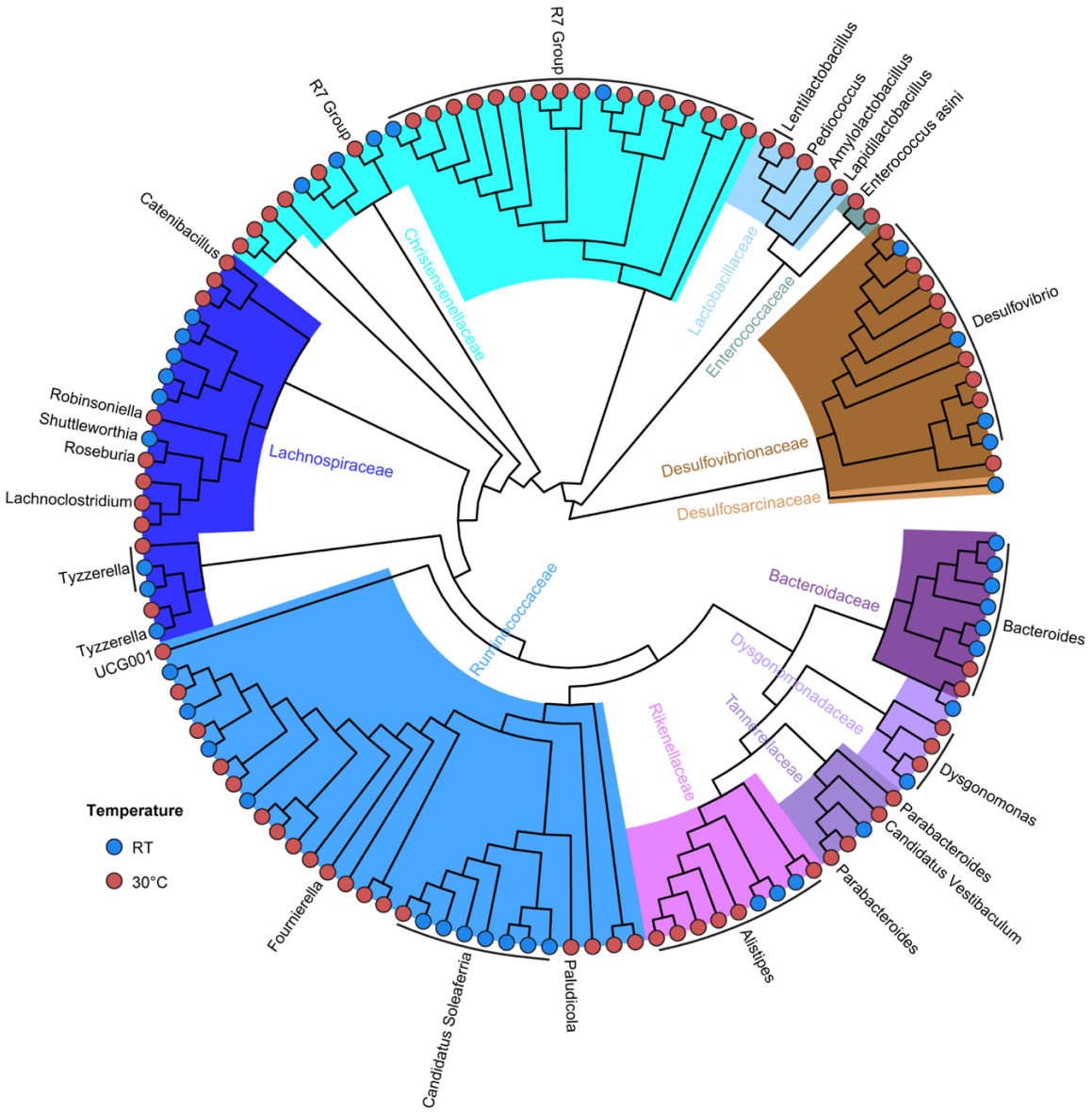

Fig 4. Phylogenetic tree of differentially abundant ASVs across temperature treatments. FastTree depicting differentially abundant ASVs in the most abundant families (maximum relative abundance > 10%). Highlights represent family level classifications. Leaf tip labels represent genus level classifications. ASVs without a leaf tip label were not classifiable at the genus level. Leaf tip colors depict which treatment ASVs were enriched in. Branch lengths not shown. RT = room temperature.

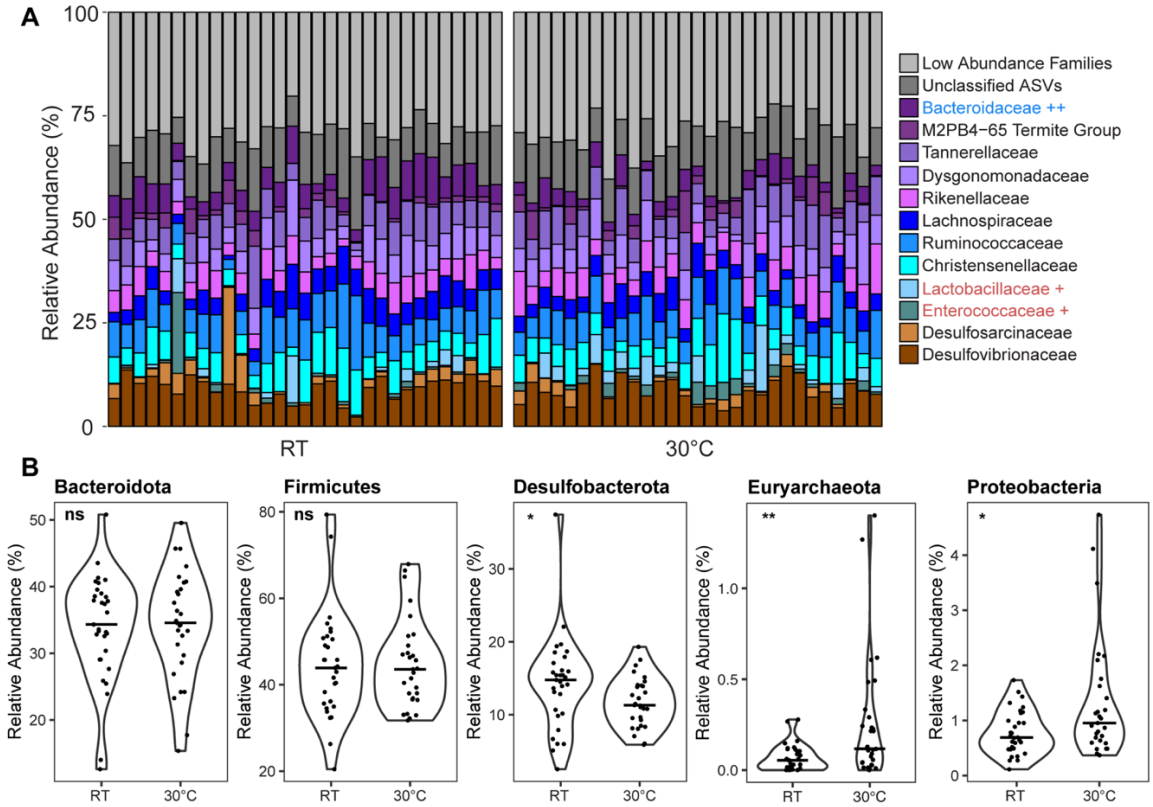

Fig 5. Comparison of family and phylum level relative abundances across temperature treatments.

(A) Relative abundance of the 12 most abundant families (maximum relative abundance > 10%). Each bar represents an individual sample. ++ = higher in room temperature treatment, + = higher in 30°C treatment. (B) Violin plots showing the relative abundance of select phyla where bars represent the median and points represent individual samples. All libraries were resampled to a depth of 10,797 reads. Wilcoxon rank-sum tests were used to compare relative abundance across temperature treatments. RT = room temperature, * = $p < 0.05$, ** = $p < 0.01$, ns = no significance.

References

1. Stork NE. How Many Species of Insects and Other Terrestrial Arthropods Are There on Earth? Annu Rev Entomol. 2018;63:31–45.

2. Whiles MR, Callaham MA, Meyer CK, Brock BL, Charlton RE. Emergence of Periodical Cicadas (Magicicada cassini) From a Kansas Riparian Forest: Densities, Biomass and Nitrogen Flux. Am Midl Nat. 2001;145(1):176–87.

3. Metcalfe DB, Asner GP, Martin RE, Silva Espejo JE, Huasco WH, Farfán Amézquita FF, et al. Herbivory makes major contributions to ecosystem carbon and nutrient cycling in tropical forests. Ecol Lett. 2014;17(3):324–32.

4. Emerson PM, Lindsay SW, Walraven GEL, Faal H, Bøgh C, Lowe K, et al. Effect of fly control on trachoma and diarrhoea. Lancet. 1999;353:1401–3.

5. Effler PV, Pang L, Kitsutani P, Vorndam V, Nakata M, Ayers T, et al. Dengue Fever, Hawaii, 2001–2002. Emerg Infect Dis. 2005;11(5):742–9.

6. Rader R, Bartomeus I, Garibaldi LA, Garratt MPD, Howlett BG, Winfree R, et al. Non-bee insects are important contributors to global crop pollination. Proc Natl Acad Sci. 2016;113(1):146–51.

7. Bowling RD, Brewer MJ, Kerns DL, Gordy J, Seiter N, Elliott NE, et al. Sugarcane Aphid (Hemiptera: Aphididae): A New Pest on Sorghum in North America. J Integr Pest Manag. 2016;7(1):12.

8. González-Tokman D, Córdoba-Aguilar A, Dáttilo W, Lira-Noriega A, Sánchez-Guillén RA, Villalobos F. Insect responses to heat: physiological mechanisms, evolution and ecological implications in a warming world. Biol Rev. 2020;95(3):802–21.

9. Toro ID, Ribbons RR, Ellison AM. Ant-mediated ecosystem functions on a warmer planet: effects on soil movement, decomposition and nutrient cycling. J Anim Ecol. 2015;84(5):1233–41.

10. Luo B, Huang M, Wang W, Niu J, Shrestha M, Zeng H, et al. Ant nests increase litter decomposition to mitigate the negative effect of warming in an alpine grassland ecosystem. Proc R Soc B. 290:20230613.

11. Temperatures Rising: NASA Confirms 2024 Warmest Year on Record - NASA [Internet]. [cited 2025]. Available from: https://www.nasa.gov/news-release/temperatures-rising-nasa-confirms-2024-warmest-year-on-record/

12. IPCC, 2023: Climate Change 2023: Synthesis Report. Contribution of Working Groups I, II and III to the Sixth Assessment Report of the Intergovernmental Panel on Climate Change [Core Writing Team, H. Lee and J. Romero (eds.)]. Geneva, Switzerland: IPCC; 2023 p. 35–115.

531 13. Atkinson D. Temperature and Organism Size—A Biological Law for Ectotherms? Adv Ecol
532 Res. 1994;25:1–58.

533 14. Mas-Martí E, Muñoz I, Oliva F, Canhoto C. Effects of increased water temperature on leaf
534 litter quality and detritivore performance: a whole-reach manipulative experiment. Freshw
535 Biol. 2015;60(1):184–97.

536 15. Garrad R, Booth DT, Furlong MJ. The effect of rearing temperature on development, body
537 size, energetics and fecundity of the diamondback moth. Bull Entomol Res.
538 2016;106(2):175–81.

539 16. Cummings JH, Pomare EW, Branch WJ, Naylor CPE, Macfarlane GT. Short chain fatty acids
540 in human large intestine, portal, hepatic and venous blood. Gut. 1987;28(10):1221–7.

541 17. Ridaura VK, Faith JJ, Rey FE, Cheng J, Duncan AE, Kau AL, et al. Gut Microbiota from
542 Twins Discordant for Obesity Modulate Metabolism in Mice. Science. 2013;341:1241214.

543 18. Kenny DJ, Plichta DR, Shungin D, Koppel N, Hall AB, Fu B, et al. Cholesterol Metabolism
544 by Uncultured Human Gut Bacteria Influences Host Cholesterol Level. Cell Host Microbe.
545 2020;28:245–57.

546 19. Reinhardt C, Bergentall M, Greiner TU, Schaffner F, Östergren-Lundén G, Petersen LC, et
547 al. Tissue factor and PAR1 promote microbiota-induced intestinal vascular remodelling.
548 Nature. 2012;483:627–31.

549 20. Gordon HA, Bruckner-Kardoss E. Effect of normal microbial flora on intestinal surface area.
550 Am J Physiol-Leg Content. 1961;201(1):175–8.

551 21. Banasaz M, Norin E, Holma R, Midtvedt T. Increased Enterocyte Production in Gnotobiotic
552 Rats Mono-Associated with *Lactobacillus rhamnosus* GG. Appl Environ Microbiol.
553 2002;68(6):3031–4.

554 22. Bouskra D, Brézillon C, Bérard M, Werts C, Varona R, Boneca IG, et al. Lymphoid tissue
555 genesis induced by commensals through NOD1 regulates intestinal homeostasis. Nature.
556 2008;456:507–10.

557 23. Sanos SL, Bui VL, Mortha A, Oberle K, Heners C, Johner C, et al. RORγt and commensal
558 microflora are required for the differentiation of mucosal interleukin 22–producing NKp46+
559 cells. Nat Immunol. 2009;10(1):83–91.

560 24. Cash HL, Whitham CV, Behrendt CL, Hooper LV. Symbiotic Bacteria Direct Expression of
561 an Intestinal Bactericidal Lectin. Science. 2006;313:1126–30.

562 25. Prado SS, Hung KY, Daugherty MP, Almeida RPP. Indirect Effects of Temperature on Stink
563 Bug Fitness, via Maintenance of Gut-Associated Symbionts. Appl Environ Microbiol.
564 2010;76(4):1261–6.

565 26. Kikuchi Y, Tada A, Musolin DL, Hari N, Hosokawa T, Fujisaki K, et al. Collapse of Insect
566 Gut Symbiosis under Simulated Climate Change. mBio. 2016;7(5):e01578-16.

567 27. McMunn MS, Hudson AI, Zemenick AT, Egerer M, Bennett L, Philpott SM, et al. Thermal
568 sensitivity and seasonal change in the gut microbiome of a desert ant, *Cephalotes rohweri*.
569 FEMS Microbiol Ecol. 2022;98(7):1–11.

570 28. Ramsby BD, Hoogenboom MO, Whalan S, Webster NS. Elevated seawater temperature
571 disrupts the microbiome of an ecologically important bioeroding sponge. Mol Ecol.
572 2018;27:2124–37.

573 29. Jokiel PL, Coles SL. Effects of temperature on the mortality and growth of Hawaiian reef
574 corals. Mar Biol. 1977;43:201–8.

575 30. Li YF, Yang N, Liang X, Yoshida A, Osatomi K, Power D, et al. Elevated Seawater
576 Temperatures Decrease Microbial Diversity in the Gut of *Mytilus coruscus*. Front Physiol.
577 2018;9:839.

578 31. Renelies-Hamilton J, Germer K, Sillam-Dussès D, Bodawatta KH, Poulsen M. Disentangling
579 the Relative Roles of Vertical Transmission, Subsequent Colonizations, and Diet on
580 Cockroach Microbiome Assembly. mSphere. 2021;6(1):e01023-20.

581 32. Cazzaniga M, Domínguez-Santos R, Marín-Miret J, Gil R, Latorre A, García-Ferris C.
582 Exploring Gut Microbial Dynamics and Symbiotic Interaction in *Blattella germanica* Using
583 Rifampicin. Biology. 2023;12(7):955.

584 33. Tinker KA, Ottesen EA. Differences in Gut Microbiome Composition Between Sympatric
585 Wild and Allopatric Laboratory Populations of Omnivorous Cockroaches. Front Microbiol.
586 2021;12:703785.

587 34. Dukes HE, Tinker KA, Ottesen EA. Disentangling hindgut metabolism in the American
588 cockroach through single-cell genomics and metatranscriptomics. Front Microbiol.
589 2023;14:1156809.

590 35. Dockman RL, Ottesen EA. Purified fibers in chemically defined synthetic diets destabilize
591 the gut microbiome of an omnivorous insect model. Front Microbiomes. 2024;3:1477521.

592 36. Jahnes BC, Poudel K, Staats AM, Sabree ZL. Microbial colonization promotes model
593 cockroach gut tissue growth and development. J Insect Physiol. 2021;133:104274.

594 37. Jahnes BC, Herrmann M, Sabree ZL. Conspecific coprophagy stimulates normal
595 development in a germ-free model invertebrate. PeerJ. 2019;7:e6914.

596 38. Turner M, Van Hulzen L, Pietri JE. The gut microbiota induces melanin deposits that act as
597 substrates for *fimA*-mediated aggregation of *Salmonella* Typhimurium and enhance infection
598 of the German cockroach vector. Microbiol Spectr. 2023;11(5):e02119-23.

599 39. Turner M, Van Hulzen L, Guse K, Agany D, Pietri JE. The gut microbiota confers resistance
600 against *Salmonella* Typhimurium in cockroaches by modulating innate immunity. iScience.
601 2024;27:111293.

602 40. Wada-Katsumata A, Zurek L, Nalyanya G, Roelofs WL, Zhang A, Schal C. Gut bacteria
603 mediate aggregation in the German cockroach. Proc Natl Acad Sci. 2015;112(51):15678–83.

604 41. Tinker KA, Ottesen EA. Phylosymbiosis across Deeply Diverging Lineages of Omnivorous
605 Cockroaches (Order Blattodea). Appl Environ Microbiol. 2020;86(7):e02513-19.

606 42. Irmler L, Furch K. Production, energy, and nutrient turnover of the cockroach *Epilampra*
607 *irmleri* Rocha e Silva & Aguiar in a Central-Amazonian inundation forest. AMAZONIANA.
608 1979;6(4):497–520.

609 43. Wang C, Lee CY, Rust MK. Biology and Management of the German Cockroach. Clayton
610 South VIC, Australia: CSIRO Publishing; 2021.

611 44. Arbes SJ, Gergen PJ, Elliott L, Zeldin DC. Prevalences of positive skin test responses to 10
612 common allergens in the US population: Results from the Third National Health and
613 Nutrition Examination Survey. J Allergy Clin Immunol. 2005;116(2):377–83.

614 45. Kang B, Vellody D, Homburger H, Yunginger JW. Cockroach cause of allergic asthma: Its
615 specificity and immunologic profile. J Allergy Clin Immunol. 1979;63(2):80–6.

616 46. Memona H, Manzoor F, Anjum AA. Cockroaches (Blattodea: Blattidae): A Reservoir of
617 Pathogenic Microbes in Human-Dwelling Localities in Lahore. J Med Entomol.
618 2017;54(2):435–40.

619 47. Liu J, Yuan Y, Feng L, Lin C, Ye C, Liu J, et al. Intestinal pathogens detected in cockroach
620 species within different food-related environment in Pudong, China. Sci Rep. 2024;14:1947.

621 48. Rosenstreich DL, Eggleston P, Kattan M, Baker D, Slavin RG, Gergen P, et al. The Role of
622 Cockroach Allergy and Exposure to Cockroach Allergen in Causing Morbidity among Inner-
623 City Children with Asthma. N Engl J Med. 1997;336(19):1356–63.

624 49. Gulati J. Pest Control in the US. IBIS World Industry Report; 2025 Nov. Report No.: 56171.

625 50. Inward D, Beccaloni G, Eggleton P. Death of an order: a comprehensive molecular
626 phylogenetic study confirms that termites are eusocial cockroaches. Biol Lett. 2007;3:331–5.

627 51. Arango RA, Schoville SD, Currie CR, Carlos-Shanley C. Experimental Warming Reduces
628 Survival, Cold Tolerance, and Gut Prokaryotic Diversity of the Eastern Subterranean
629 Termite, *Reticulitermes flavipes* (Kollar). Front Microbiol. 2021;12:632715.

630 52. Arango RA, Bishell AB, Ohno KM, Shelton TG, Schoville SD, Carlos-Shanley C. Seasonal
631 shifts in gut microbiota and cold tolerance metrics in a northern population of *Reticulitermes*
632 *flavipes* (Blattodea: Rhinotermitidae). Environ Entomol. 2024;53(3):447–56.

633 53. Gunn DL. The Temperature and Humidity Relations of the Cockroach: III. A Comparison of
634 Temperature Preference, and Rates of Desiccation and Respiration of *Periplaneta*
635 *Americana*, *Blatta Orientalis* and *Blatella Germanica*. J Exp Biol. 1935;12(2):185–90.

636 54. Ayayee PA, Ondrejech A, Keeney G, Muñoz-Garcia A. The role of gut microbiota in the
637 regulation of standard metabolic rate in female *Periplaneta americana*. PeerJ. 2018;6:e4717.

638 55. Lee S, Kim JY, Yi MH, Lee IY, Lee WJ, Moon HS, et al. Comparative Microbiome Analysis
639 of Three Species of Laboratory-Reared *Periplaneta* Cockroaches. Korean J Parasitol.
640 2020;58(5):537–42.

641 56. Vera-Ponce de León A, Jahnes BC, Otero-Bravo A, Sabree ZL. Microbiota Perturbation or
642 Elimination Can Inhibit Normal Development and Elicit a Starvation-Like Response in an
643 Omnivorous Model Invertebrate. mSystems. 2021;6:e00802-21.

644 57. Chen Z, Wen S, Shen J, Wang J, Liu W, Jin X. Composition and diversity of the gut
645 microbiota across different life stages of American cockroach (*Periplaneta americana*). Bull
646 Entomol Res. 2023;1–7.

647 58. Bertino-Grimaldi D, Medeiros MN, Vieira RP, Cardoso AM, Turque AS, Silveira CB, et al.
648 Bacterial community composition shifts in the gut of *Periplaneta americana* fed on different
649 lignocellulosic materials. SpringerPlus. 2013;2:609.

650 59. Zurek L, Keddie BA. Contribution of the colon and colonic bacterial flora to metabolism and
651 development of the American cockroach *Periplaneta americana* L. J Insect Physiol.
652 1996;42(8):743–8.

653 60. Rollo CD, Gunderman MW. Variation among individuals and the effect of temperature on
654 food consumption and reproduction in the cockroach, *Periplaneta americana* (Orthoptera:
655 Blattidae). Can Entomol. 1984;116(6):785–93.

656 61. Nadkarni MA, Martin FE, Jacques NA, Hunter N. Determination of bacterial load by real-
657 time PCR using a broad-range (universal) probe and primers set. Microbiology.
658 2002;148:257–66.

659 62. Wickham H, Averick M, Bryan J, Chang W, McGowan LD, François R, et al. Welcome to
660 the Tidyverse. J Open Source Softw. 2019;4(43):1686.

661 63. Tinker KA, Ottesen EA. The Core Gut Microbiome of the American Cockroach, *Periplaneta*
662 *americana*, Is Stable and Resilient to Dietary Shifts. Appl Environ Microbiol.
663 2016;82(22):6603–10.

664 64. Callahan BJ, McMurdie PJ, Rosen MJ, Han AW, Johnson AJA, Holmes SP. DADA2: High-
665 resolution sample inference from Illumina amplicon data. Nat Methods. 2016;13(7):581–3.

666 65. Quast C, Pruesse E, Yilmaz P, Gerken J, Schweer T, Yarza P, et al. The SILVA ribosomal
667 RNA gene database project: improved data processing and web-based tools. Nucleic Acids
668 Res. 2013;41:D590–6.

66. R Core Team. R: A Language and Environment for Statistical Computing [Internet]. Vienna, Austria: R Foundation for Statistical Computing; 2022. Available from: https://www.R-project.org/

67. Oksanen J, Simpson GL, Blanchet FG, Kindt R, Legendre P, Minchin PR, et al. vegan: Community Ecology Package [Internet]. 2022. Available from: https://cran.r-project.org/web/packages/vegan/index.html

68. Legendre P, De Cáceres M. Beta diversity as the variance of community data: dissimilarity coefficients and partitioning. Ecol Lett. 2013;16:951–63.

69. Love MI, Huber W, Anders S. Moderated estimation of fold change and dispersion for RNA-seq data with DESeq2. Genome Biol. 2014;15:550.

70. Sievers F, Wilm A, Dineen D, Gibson TJ, Karplus K, Li W, et al. Fast, scalable generation of high-quality protein multiple sequence alignments using Clustal Omega. Mol Syst Biol. 2011;7:539.

71. Price MN, Dehal PS, Arkin AP. FastTree: Computing Large Minimum Evolution Trees with Profiles instead of a Distance Matrix. Mol Biol Evol. 2009;26(7):1641–50.

72. Price MN, Dehal PS, Arkin AP. FastTree 2 – Approximately Maximum-Likelihood Trees for Large Alignments. PLOS ONE. 2010;5(3):e9490.

73. Yu G, Smith DK, Zhu H, Guan Y, Lam TTY. ggtree: an R package for visualization and annotation of phylogenetic trees with their covariates and other associated data. Methods Ecol Evol. 2017;8:28–36.

74. Gu Z. Complex heatmap visualization. iMeta. 2022;1:e43.

75. Gu Z, Eils R, Schlesner M. Complex heatmaps reveal patterns and correlations in multidimensional genomic data. Bioinformatics. 2016;32(18):2847–9.

76. Ogle DH, Doll JC, Wheeler AP, Dinno A. FSA: Simple Fisheries Stock Assessment Methods [Internet]. 2025. Available from: https://CRAN.R-project.org/package=FSA

77. Horváthová T, Babik W, Kozłowski J, Bauchinger U. Vanishing benefits - The loss of actinobacterial symbionts at elevated temperatures. J Therm Biol. 2019;82:222–8.

78. Berg M, Stenuit B, Ho J, Wang A, Parke C, Knight M, et al. Assembly of the *Caenorhabditis elegans* gut microbiota from diverse soil microbial environments. ISME J. 2016;10:1998–2009.

79. Ferguson LV, Dhakal P, Lebenzon JE, Heinrichs DE, Bucking C, Sinclair BJ. Seasonal shifts in the insect gut microbiome are concurrent with changes in cold tolerance and immunity. Funct Ecol. 2018;32:2357–68.

80. Moghadam NN, Thorshauge PM, Kristensen TN, De Jonge N, Bahrndorff S, Kjeldal H, et al. Strong responses of *Drosophila melanogaster* microbiota to developmental temperature. Fly (Austin). 2018;12(1):1–12.

81. Willing B, Halfvarson J, Dicksved J, Rosenquist M, Järnerot G, Engstrand L, et al. Twin Studies Reveal Specific Imbalances in the Mucosa-associated Microbiota of Patients with Ileal Crohn's Disease. Inflamm Bowel Dis. 2009;15(5):653–60.

82. Willing BP, Dicksved J, Halfvarson J, Andersson AF, Lucio M, Zheng Z, et al. A Pyrosequencing Study in Twins Shows That Gastrointestinal Microbial Profiles Vary With Inflammatory Bowel Disease Phenotypes. Gastroenterology. 2010;139:1844–54.

83. Su Q, Tun HM, Liu Q, Yeoh YK, Mak JWY, Chan FKL, et al. Gut microbiome signatures reflect different subtypes of irritable bowel syndrome. Gut Microbes. 2023;15(1):2157697.

84. Dahal RH, Kim S, Kim YK, Kim ES, Kim J. Insight into gut dysbiosis of patients with inflammatory bowel disease and ischemic colitis. Front Microbiol. 2023;14:1174832.

85. Pietrucci D, Cerroni R, Unida V, Farcomeni A, Pierantozzi M, Mercuri NB, et al. Dysbiosis of gut microbiota in a selected population of Parkinson's patients. Parkinsonism Relat Disord. 2019;65:124–30.

86. Zaneveld JR, McMinds R, Thurber RV. Stress and stability: applying the Anna Karenina principle to animal microbiomes. Nat Microbiol. 2017;2:17121.

87. Ma Z. Testing the Anna Karenina Principle in Human Microbiome-Associated Diseases. iScience. 2020;23:101007.

88. DePoy AN, Wall HE, Tinker KA, Black IM, Ottesen EA. Metabolic flexibility among fiber degraders supports gut microbiome stability across host diets in the American cockroach [Internet]. bioRxiv; 2025 [cited 2026]. p. 2024.10.31.621369. Available from: https://www.biorxiv.org/content/10.1101/2024.10.31.621369v3

89. Gibson GR, Cummings JH, Macfarlane GT. Competition for hydrogen between sulphate-reducing bacteria and methanogenic bacteria from the human large intestine. J Appl Bacteriol. 1988;65:241–7.

90. Lovley DR, Dwyer DF, Klug MJ. Kinetic Analysis of Competition Between Sulfate Reducers and Methanogens for Hydrogen in Sediments. Appl Environ Microbiol. 1982;43(6):1373–9.

91. Bodegom PMV, Stams AJM. Effects of alternative electron acceptors and temperature on methanogenesis in rice paddy soils. Chemosphere. 1999;39(2):167–82.

92. Muller E, Guélard J, Sissmann O, Tafit A, Poirier S. Evidencing the influence of temperature and mineralogy on microbial competition for hydrogen consumption: Implications for underground hydrogen storage (UHS). Int J Hydrog Energy. 2024;82:1101–13.

93. Jung H, Kim J, Lee C. Temperature Effects on Methanogenesis and Sulfidogenesis during Anaerobic Digestion of Sulfur-Rich Macroalgal Biomass in Sequencing Batch Reactors. Microorganisms. 2019;7:682.

94. Todaka N, Moriya S, Saita K, Hondo T, Kiuchi I, Takasu H, et al. Environmental cDNA analysis of the genes involved in lignocellulose digestion in the symbiotic protist community of *Reticulitermes speratus*. FEMS Microbiol Ecol. 2007;59:592–9.

95. Gijzen HJ, Barugahare M. Contribution of anaerobic protozoa and methanogens to hindgut metabolic activities of the American cockroach, *Periplaneta americana*. Appl Environ Microbiol. 1992;58(8):2565–70.

96. Bai TT, Pei XJ, Liu TX, Fan YL, Zhang SZ. Melanin synthesis genes *BgTH* and *BgDdc* affect body color and cuticle permeability in *Blattella germanica*. Insect Sci. 2022;29:1552–68.

97. Bennett AF, Lenski RE. Evolutionary Adaptation to Temperature II. Thermal Niches of Experimental Lines of *Escherichia Coli*. Evolution. 1993;47(1):1–12.